

TECHNICAL REPORT

Le présent document a été reproduit
avec l'autorisation de CANCOPY.
Tous les autres réprints ou reproductions ultérieures
en sont strictement interdites.

Analysis of Mixed Oxide Fuel Loaded Cores in the Heavy Water Reactor FUGEN

Tsukasa OHTANI^{1,*†}, Takashi IJIMA¹ and Yoshitake SHIRATORI²

¹Fugen Nuclear Power Station, Tsuruga Head Office, Japan Nuclear Cycle Development Institute,
Myojin-cho, Tsuruga-shi, Fukui 914-8510

²Tokyo Office, Japan Nuclear Cycle Development Institute, Uchisaiwai-cho, Chiyoda-ku, Tokyo 100-8577

(Received March 27, 2003 and accepted in revised form August 7, 2003)

Uranium-plutonium mixed oxide (MOX) fuel cores in the heavy water reactor, FUGEN, were analyzed using the Advanced Thermal Reactor (ATR) type core design code system WIMS-ATR/POLESTAR and the accuracy of this code system also has been evaluated by means of operational data through the 34 burnup cycles and on-site γ -scanning data. The root mean square errors of calculated thermal neutron flux distributions were less than 5% compared with the power calibration monitor traverse data. The root mean square error of calculated power distributions was less than 4% compared with the γ -scanning data. The root mean square error of calculated burnup distributions was less than 3% compared with the γ -scanning data. The averaged effective multiplication factor was 1.000 and its standard deviation was 0.002. The calculation accuracy of void reactivity coefficient was $\pm 3 \times 10^{-5} \Delta k/k/\% \text{void}$ for the equilibrium cores. The calculation accuracy of power coefficient was $\pm 1.5 \times 10^{-5} \Delta k/k/\% \text{power}$. The accuracy of ATR type core design code system was enough for the core management in the Fugen Nuclear Power Station.

KEYWORDS: Fugen, MOX fuel, advanced thermal reactor, heavy water reactor, core design code, modern nodal method, WIMS-ATR, POLESTAR

I. Introduction

The prototype Advanced Thermal Reactor (ATR), FUGEN, was the first thermal reactor to demonstrate the full-scale utilization of uranium-plutonium mixed oxide (MOX) fuel assemblies in the world.¹⁾ The total number of 772 MOX fuel assemblies has been loaded in the core, which is the largest MOX fuel utilization at any single thermal reactor in the world.

In FUGEN, it is possible to load MOX fuel assemblies in the full core, but in fact, its loading ratio has been flexibly changed from 34 to 72% according to the supply and demand circumstances of plutonium.

FUGEN has played the leading role in the nuclear fuel cycle and established the domestic basis for plutonium utilization, in both technological and political terms, for 25 years operation period.

In ATR, the fission neutrons are well moderated mainly in the heavy water and the moderated thermal neutrons are supplied to the fuel assemblies so that it is possible to use the MOX fuel like UO_2 fuel.

For the purpose of ATR type core design code system's accuracy improvement, it is taken account of the differences of isotopic composition of the plutonium, ^{241}Pu β -decay, and ^{241}Am accumulation. Furthermore, the modern nodal method with JENDL-3.2 nuclear data library is installed in this code system for the purpose of additional accuracy improvement.

The accuracy of this code system also has been evaluated by means of operational data such as thermal neutron flux

distributions, on-site γ -scanning data, effective multiplication factor, void reactivity coefficient and power coefficient.

II. Plant Description

1. Reactor Core

FUGEN is a 165MW electrical output, heavy water moderated, boiling light water cooled, pressure tube type reactor. The main reactor core data are listed in Table 1 and a schema of the reactor core is shown in Fig. 1. The reactor consists of a calandria tank, pressure tubes, control rods, iron and water shields, etc.

The heavy water moderator is contained in a calandria tank, in which 224 pressure tubes are installed vertically. One fuel assembly is installed in each pressure tube, in which light water flows as a coolant. The pressure tube is surrounded by calandria tube so that the heavy water moderator and light

Table 1 Reactor core data

Item	Specification
Reactor type	Heavy water moderated, boiling light water cooled, pressure tube type
Thermal output	557 MW
Electrical output	165 MW
Core height	3.7 m
Core diameter	4.05 m
Coolant pressure	68 kg/cm ² -a
Coolant flow rate	7,600 t/h
Number of fuel assemblies	224
Number of control rods	49
Moderator (D_2O) inventory	160 t

*Corresponding author, Tel. +81-3-3546-2211, Fax. +81-3-3546-2805, E-mail: Tsukasa.Ootani@jpower.co.jp

†Present address: Electric Power Development Co., Ltd., Ginza, Chuo-ku, Tokyo 104-8165

water coolant are completely separated. There are 49 control rods, which are inserted from the reactor top into the heavy water *via* guide tubes installed in the calandria tank. The heavy water is cooled to maintain its fixed temperature at reactor entrance and, ^{10}B is added to the heavy water to control the burnup reactivity in the core. The calandria tank is surrounded by the iron and water shield for shielding the neutron and the γ -ray from the reactor core.

2. Fuel Assembly

The standard fuel specifications are listed in Table 2, and a schema of the standard fuel assembly is shown in Fig. 2. The standard fuel assembly consists of 28 fuel rods (inner: 4 rods, intermediate: 8 rods, and outer: 16 rods) and its form is cylindrical cluster so that it can be inserted into a pressure tube. The total length of the standard fuel assembly is 4.4 m (the meat length: 3.7 m).

There are four types of standard fuel assemblies (MOX fuel type A and type B with different fissile contents, and UO_2 fuel type A and type B with different enrichment). The type A fuel, which contains lower fissile materials (1.4 wt% fissile for MOX and 1.5 wt% enrichment for UO_2), was used for the initial core and the type B fuel, which contains higher fissile materials (2.0 wt% fissile for MOX and 1.9 wt% enrichment for UO_2), has been used for equilibrium core. Besides these standard fuel assemblies, four special UO_2 fuel assemblies, which contain specimens of the pressure tube material for the purpose of irradiation tests, are also loaded into the center region in the core and its position is fixed.

Furthermore, the other four types of test MOX fuel assemblies (36 rods fuel, Gd type I, Gd type II and segment fuel) were loaded in FUGEN. The 36 rods fuel was produced for the performance test of the demonstration ATR fuel. The Gd type I and Gd type II, which contain UO_2 pellet with

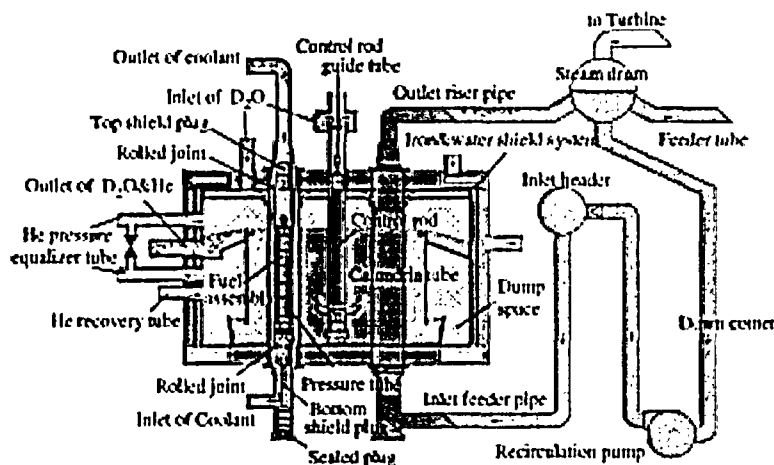


Fig. 1 Illustration of the reactor core

Table 2 Standard fuel specifications

		MOX fuel		UO_2 fuel	
		Type A	Type B	Type A	Type B
Pellet	Diameter	14.4 mm		14.4 mm	
	Density	95%TD		95%TD	
	Fissile content (wt%)	1.4	2.0	1.5	1.9
	Material	Zircaloy-2			
Clad	Outer diameter	16.5 mm			
	Thickness	0.9 mm			
Rod	Meat length	3.7 m			
	He pressure	1.0 kg/cm ² ·a			
Assembly	Form	Cylindrical cluster			
	Total length	4.4 m			
	Outer diameter	112 mm			
	Number of rods	28			
Design condition	Maximum burnup	20,000 MWd/t			
	Maximum LHGR	574 W/cm (17.5 kW/ft)			

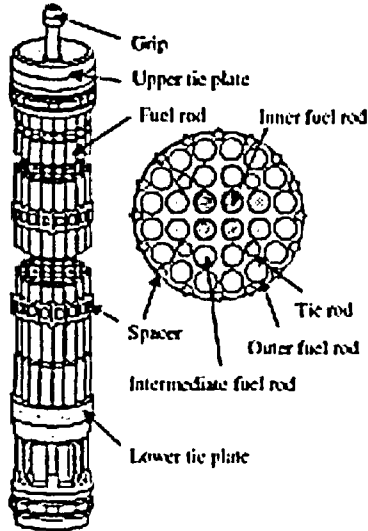


Fig. 2 Standard fuel assembly

Gd₂O₃, were produced for the confirmation of the high burnup demonstration ATR fuel's safety and the gadolinia fuel's irradiation characteristics. The density of Gd₂O₃ is 0.8 wt% to 1.4 wt% for Gd type I and 0.7 wt% to 1.2 wt% for Gd type II. The segment fuel, in which the short length fuel rods are built in and it consists of zirconium liner clad, hollow pellet, etc., was produced as a part of the high performance fuel developments. After the irradiation in Fugen, these test MOX fuel assemblies were discharged for the purpose of post-irradiation examinations or power ramp tests.

III. Core Characteristics and Core Layout

1. Core Characteristics

The main characteristics of FUGEN's core²⁻⁶⁾ are as follows.

(1) MOX Fuel can be used the same as UO₂ Fuel

The fission neutrons are well moderated mainly in the heavy water, and the neutron spectrum is softer than that of LWR. The moderated thermal neutrons are supplied to the MOX fuel assemblies so that it is possible to avoid the resonance peak (shown in Fig. 3). Furthermore, the averaged neutron yield per absorption (η) of the fissile plutonium (²³⁹Pu and ²⁴¹Pu) is nearly equal to that of ²³⁵U (shown in Fig. 4). Therefore, even though isotopic compositions of the plutonium recovered from spent fuel assemblies are dissimilar, MOX fuel assemblies can be burnt approximately same way as long as the fissile content (fissile plutonium+²³⁵U) is fixed.

(2) Control Rod Worth Reduction by MOX Fuel Loading is Little

The core reactivity is controlled by 49 control rods and by ¹⁰B in the heavy water. Almost every control rods are withdrawn in full power operation, in which four automatic control rods are inserted partially into the core for the purpose of core reactivity control. The control rods are inserted into the heavy water, in which abundant thermal neutrons exist, so that the control rod worth reduction by MOX fuel loading is little.

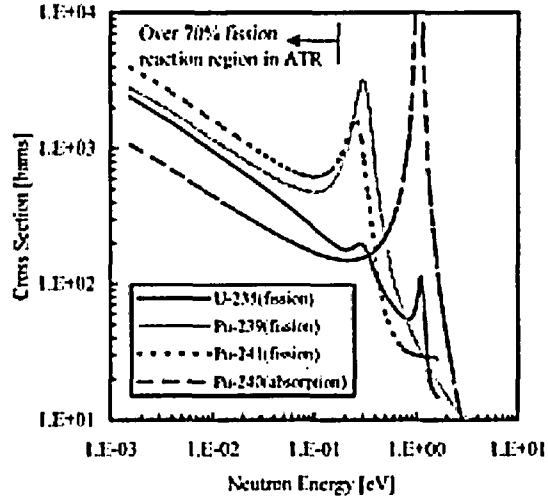


Fig. 3 Cross section of ²³⁵U and plutonium

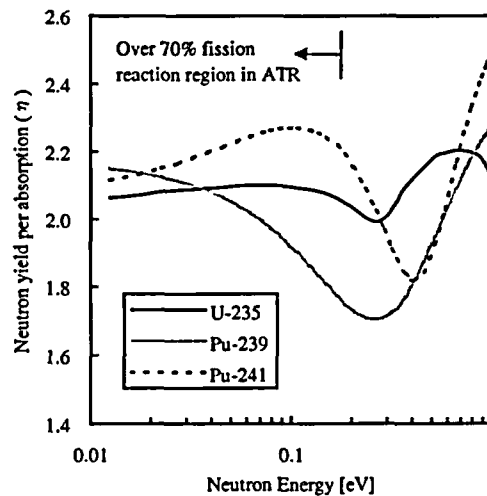


Fig. 4 Neutron yield per absorption of ²³⁵U and plutonium

(3) Void Reactivity Coefficient is Nearly Zero

The thermal neutron absorption by the light water is bigger than that of the heavy water, in the sight of effective utilization of thermal neutrons, so that the light water volume is optimized to the minimum for cooling the fuel. Therefore, the effects of moderation and absorption are balanced in the coolant region so that the void reactivity coefficient is nearly zero in the core. The measurement of void reactivity coefficient was $\pm 5 \times 10^{-5} \Delta k/k/\% \text{void}$ for the equilibrium cores. In FUGEN, void reactivity coefficient at about 40% power level is obtained by analyzing the transient behavior of the reactor power when the reactor recirculation pump (RCP) speed changes from 450 to 900 rpm (see Sec. IV-2(4)).

2. Typical Core Layout

The typical core layout is shown in Fig. 5. As mentioned above, MOX fuel can be used like UO₂ fuel so that the loading position of MOX fuel is not fixed in the core. As a rule, a scat-

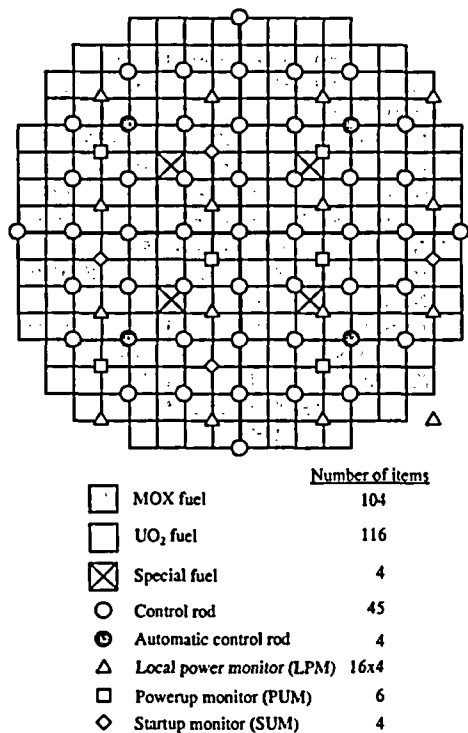


Fig. 5 Typical core layout (31th cycle)

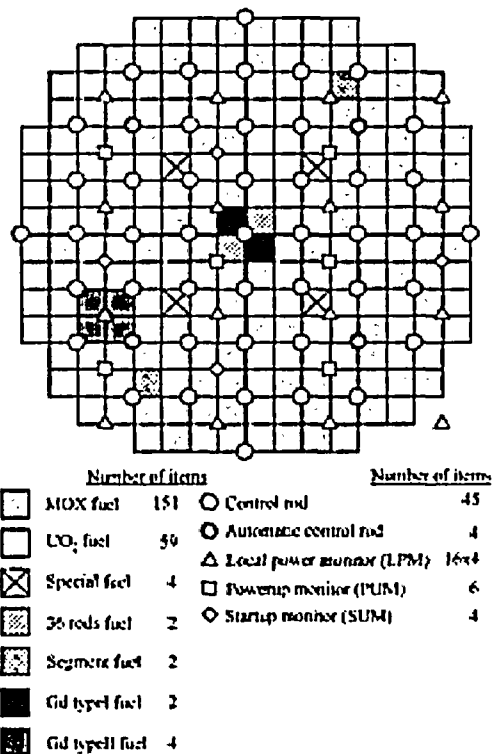


Fig. 6 Test MOX fuel loaded core layout (16th cycle)

ter loading scheme with quadrant symmetry is adopted. The basic operation period is six months with the number of 36 to 40 refueling (averaged discharge burnup: 17 GWd/t). During full power operation, transient reactivity is mainly controlled by automatic control rod and the reactivity loss caused by the fuel burnup is compensated by the removal of ¹⁰B from the heavy water.

In the 16th cycle core (shown in Fig. 6), the number of MOX fuel assemblies is 161 and the ratio of MOX fuel loading to the core is 72% (the maximum value through the 25 years operation period). For the purpose of fuel development for ATR demonstration reactor, four types of test MOX fuel assemblies (36 rods fuel, Gd type I, Gd type II and segment fuel) are loaded in the 16th cycle core. The burnup characteristics of standard fuel assemblies and test MOX fuel assemblies are shown in Fig. 7. The target burnup and the irradiation conditions (e.g. linear heat generating ratio) are different between standard fuel assemblies and test MOX fuel assemblies so that it was taken account of the control rods pattern adjustment to satisfy the thermal limitation. The results of thermal limitation of 16th cycle core are shown in Fig. 8.

IV. Development of Core Design Code System

1. Core Design Code System WIMS-ATR/POLESTAR

Core design is performed by using WIMS-ATR/POLESTAR code system (i.e., WIMS-ATR code for lattice calculation and POLESTAR code for core calculation).

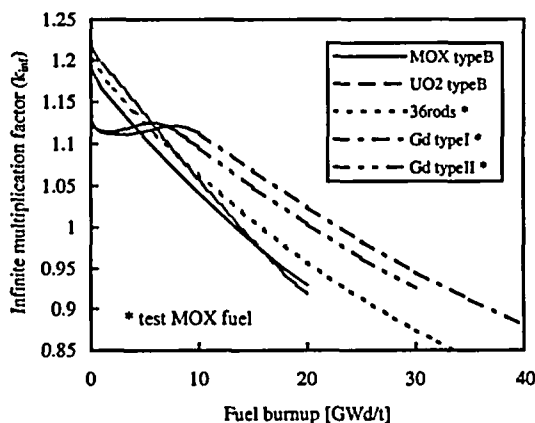


Fig. 7 Infinite multiplication factor of standard fuels and test MOX fuels

(1) Lattice Calculation Code WIMS-ATR

The WIMS-ATR code, the original code WIMS-D with UKAEA nuclear data library was developed in the United Kingdom for steam generating heavy water reactors, is 69 energy group for UKAEA library and 172 energy group for JENDL-3.2 library,⁷⁾ two-dimensional, collision probability method lattice calculation code.⁸⁾ This code was developed for use in the ATR type reactor and has been improved by use of the data from Deuterium Critical Assembly (DCA) at JNC O-arai Engineering Center and FUGEN itself. The con-

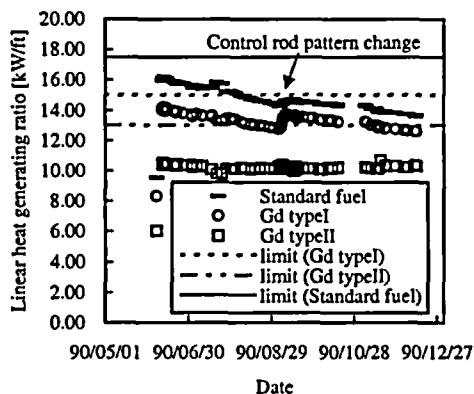


Fig. 8 Linear heat generating ratio (LHGR) of the 16th cycle

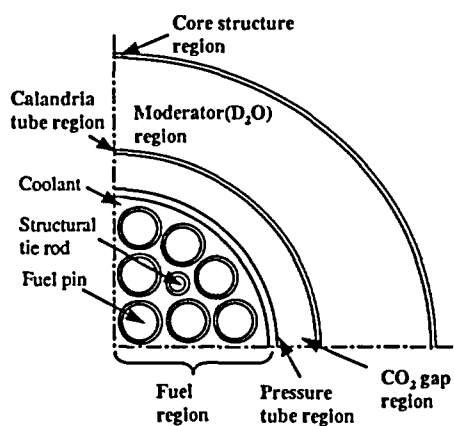


Fig. 9 Lattice calculation model for the standard fuel

crete improvements are employment of heavy water collision cross section in which temperature dependency by Honeck model⁹⁾ is considered and the addition of gadolinium nuclide cross section. This code calculates flux and power distributions in the fuel bundle cell such as group constants, infinite multiplication factor, local power peaking, isotopic compositions, reaction rates, etc. The calculated group constants are then collapsed to two energy group lattice constants and stored in the data library of the POLESTAR code. The calculation model is shown in Fig. 9 and the calculation flow is shown in Fig. 10.

(2) Core Calculation Code POLESTAR

The POLESTAR code, developed for use in the FUGEN, is a two-energy group, three-dimensional, thermonuclear coupled core calculation code in which the thermal hydraulic data of cylindrical cluster fuel assemblies from 14MW Heat Transfer Loop (HTL) at JNC O-arai Engineering Center such as void-quality correlation equation are used.^{10,11)} The solution of this code employs the finite difference method with coarse-mesh and the modern nodal method with discontinuity factor in which analytic nodal model is employed and fuel pin power distribution is calculated by multiplication of averaged node power distribution and local peaking factor. The size of radial direction calculation mesh for finite difference method and

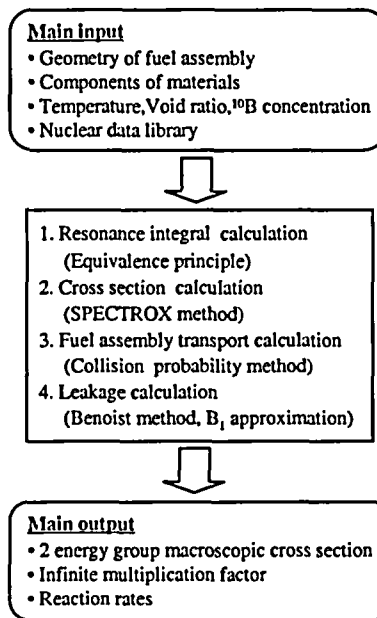


Fig. 10 Lattice calculation flow of WIMS-ATR

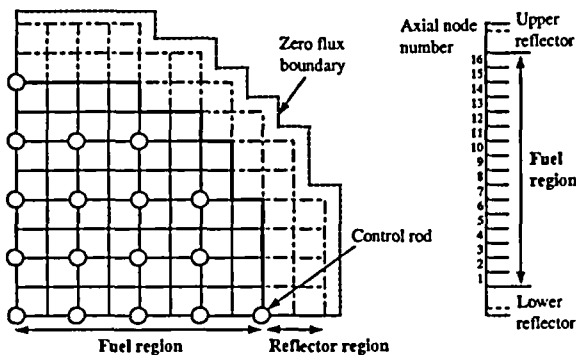


Fig. 11 Core calculation model of POLESTAR

modern nodal method is 24 cm (fuel bundle diameter). The two energy group lattice constants are different from finite difference method in which the lattice constants are calculated by WIMS-ATR with 69 energy group UKAEA library and modern nodal method in which the lattice constants are calculated by WIMS-ATR with 172 energy group JENDL-3.2 library. This code calculates power and burnup distributions in the core and also calculates the nuclear and thermal hydraulic conditions of the core such as effective multiplication factor, thermal flux, coolant void fraction, linear heat generating ratio (LHGR), rod worth, void reactivity and critical ¹⁰B concentration, etc. Furthermore, this code can calculate the xenon dynamic characteristics. The calculation model is shown in Fig. 11 and the calculation flow is shown in Fig. 12.

2. The Accuracy of the Core Design Code System

(1) Thermal Neutron Flux Distribution of the Core

The thermal neutron flux has been constantly monitored by four local power monitors (LPMs) in each of 16 channels (64

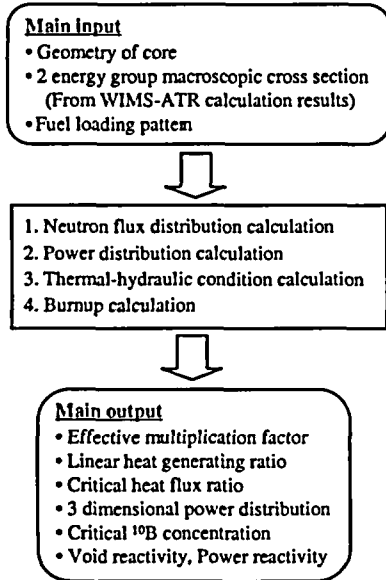


Fig. 12 Core calculation flow of POLESTAR

monitors) and also by the power calibration monitor (PCM), which is regularly inserted in the LPM channels for calibration (see Fig. 5). Hence, thermal neutron flux distributions are measured by the PCM at locations in which the operating core physics data can be directly compared with the calculations.

The PCM scanning thimbles are located in the heavy water moderator and at centers of diagonals between four fuel channels. The PCM detector is a ²³⁵U micro fission chamber and, therefore, the measurement actually corresponds to the thermal neutron density distribution considering the 1/v character of the detector. However, the density distribution and the flux distribution are almost the same over the region in which the neutron spectrum does not vary much, and here the measurement is customarily called the thermal neutron flux distribution. The calculated fuel cell average thermal fluxes have been converted to values at the PCM location by the following relation:

$$\phi_{PCM}^T = \frac{1}{4} \sum_{i=1}^4 C_i \phi_i,$$

- where ϕ_{PCM}^T : Thermal neutron flux to be compared at the PCM locations
 ϕ_i : Fuel cell average thermal neutron flux at the *i*-th channel
 C_i : Ratio of the calculated outer edge flux to fuel cell average flux in the *i*-th fuel cell, given in terms of fuel type, burnup, and ¹⁰B concentration in heavy water
i: Designation of four fuel channels surrounding PCM locations.

Typical comparison of measured and calculated thermal flux distribution is shown in Fig. 13, in which the thermal neutron flux is distorted at No. 9 axial node because of the existence of seismic protection plate. The accuracy of the

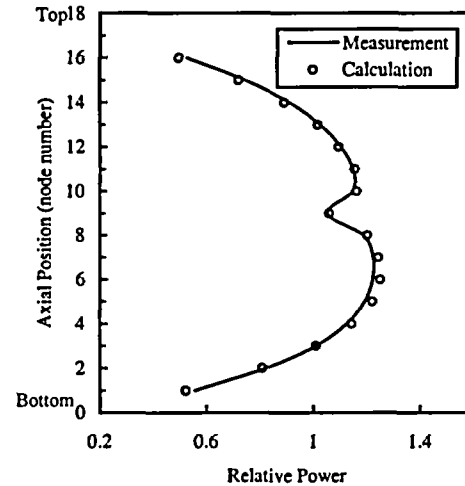


Fig. 13 Typical axial thermal flux distribution (31th cycle BOC)

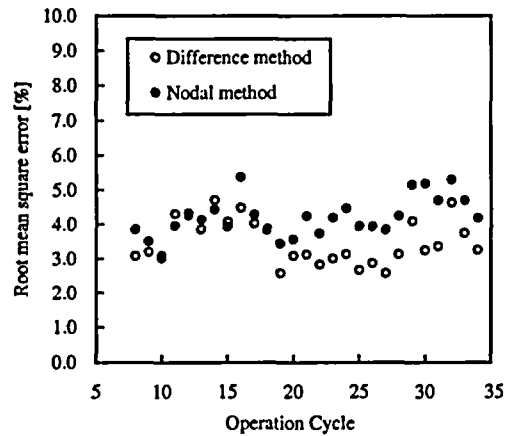


Fig. 14 Comparison of rms errors of thermal flux distribution between difference method and nodal method

POLESTAR code for thermal flux distribution is shown in Fig. 14, in which two kinds of solution, finite difference method and modern nodal method, are evaluated. Through the operation cycles, the root mean square (rms) error of the calculated thermal fluxes with respect to the measurements was within 5% for all three dimensional spatial nodes in various MOX core conditions. The accuracy of the POLESTAR code for thermal flux distribution is better than that of off-line code of process computer in which the rms error of the calculated thermal fluxes with respect to the measurements was about 10%.

In FUGEN's MOX core design, following corrections are considered, which are effects of plutonium composition difference on lattice constant and the excess reactivity reduction depends on ²⁴¹Pu β -decay and ²⁴¹Am accumulation.

(a) Correction Factor for Differences of Isotopic Composition of the Plutonium

For the purpose of considering the effects of plutonium composition difference on lattice constant, the plutonium

composition correction factor, which is defined by the ratio of lattice constant with arbitrary plutonium composition and lattice constant with basic plutonium composition, is installed:

$$\kappa(\text{Pu}, E) = \frac{\sum(\text{Pu}, E)}{\sum(\text{Basic Pu}, E)},$$

where $\kappa(\text{Pu}, E)$: Plutonium composition correction factor
 $\sum(\text{Pu}, E)$: Lattice constant with arbitrary plutonium isotopic composition
 $\sum(\text{Basic Pu}, E)$: Lattice constant with basic plutonium isotopic composition
 E : Fuel burnup.

(b) Correction Factor for ^{241}Pu β -decay and ^{241}Am Accumulation

For the purpose of considering the excess reactivity reduction, the correction factor for ^{241}Pu β -decay and ^{241}Am accumulation, which is defined by the ratio of lattice constant, in which the history of fabrication to loading and reactor shutdown period are experienced, and basic lattice constant, is installed:

$$f(T, T_c, E) = \frac{\sum(T, T_c, E)}{\sum(E)},$$

where $f(T, T_c, E)$: Correction factor for ^{241}Pu β -decay and ^{241}Am accumulation
 $\sum(T, T_c, E)$: Lattice constant with the history of fabrication to loading and reactor shutdown period
 $\sum(E)$: Basic lattice constant
 E : Fuel burnup.

(2) Power and Burnup Distribution of Fuel Assembly

The additional evaluation of POLESTAR code was carried out by means of γ -scanning for the discharged fuel assemblies. The power and burnup distribution of fuel assemblies could be measured by γ -scanning. After the 15th cycle operation, power and burnup distribution of twelve standard fuel assemblies were measured (power distribution: six fuel assemblies and burnup distribution: six fuel assemblies). The different irradiation condition's fuel assemblies were selected to measure such as fuel type, burnup, neighboring fuel assemblies to the control rod, loading position (see Table 3 and Fig. 15). Furthermore, after the 16th cycle operation, six test MOX fuel assemblies (Gd type I: four fuel assemblies and Gd type II: two fuel assemblies) and two UO_2 fuel assemblies were measured (see Table 3 and Fig. 16).

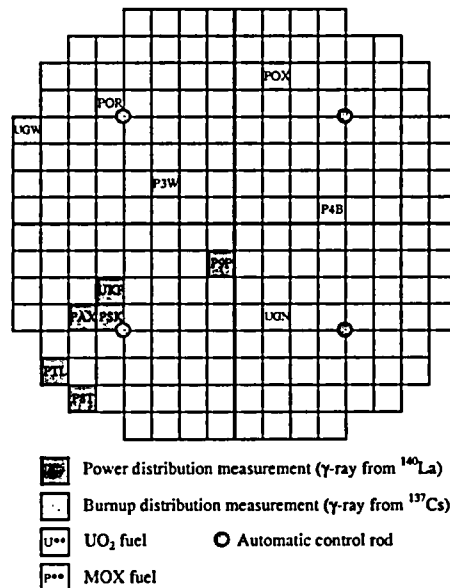


Fig. 15 The γ -scanning target fuels loaded position (15th cycle)

(a) The on-site γ -scanning System and Measuring Nuclide

The on-site γ -scanning system is shown in Fig. 17. This system mainly consists of γ -ray detector, camera, collimator and cradle, which is used at spent fuel storage pool. The γ -scanning was carried out according to the following procedures. Firstly, the fuel assembly is set in fuel inspection equipment. Secondly, the fuel assembly is moved to axial direction and rotated in order to measure the power and burnup distribution.

The ^{140}La was selected in order to measure the power distribution because ^{140}La is short half-life nuclide so that the γ -ray intensity presents the nuclear reaction before the reactor shut down. The ^{137}Cs was selected in order to measure the burnup distribution because ^{137}Cs is long half-life nuclide so that the γ -ray intensity presents the burnup history.

(b) Comparison of γ -scanning Data and Calculated Value
 a) Evaluation of POLESTAR Code by 15th Cycle γ -scanning Data

The rms errors of calculated axial power and burnup distribution with respect to the measurement are shown in Figs. 18

Table 3 The burnup of target fuels for γ -scanning

		15th cycle		16th cycle			
	Name	Burnup (GWd/t)	Name	Burnup (GWd/t)	Name	Burnup (GWd/t)	
Power distribution	PSK	7.0	POX	18.8	E08	4.2	
	PAX	11.7	UGW	14.0	E09	4.2	
	PTL	4.1	Burnup distribution	P3W	14.3	E10	3.9
	P8T	17.5	UGN	17.7	Power distribution	E11	3.5
	UKP	16.3	P4B	17.2	E12	3.3	
	P9P	18.5	POR	12.9	E13	3.7	
					UMJ	4.2	
					UMZ	4.1	

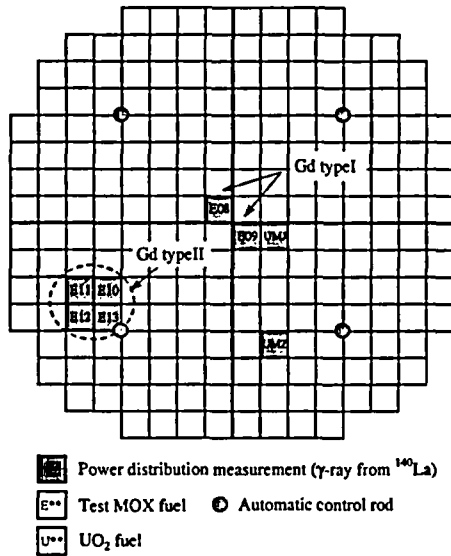


Fig. 16 The γ -scanning target fuels loaded position (16th cycle)

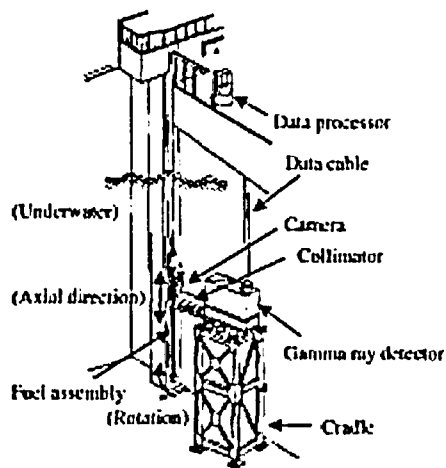


Fig. 17 Illustration of γ -scanning system

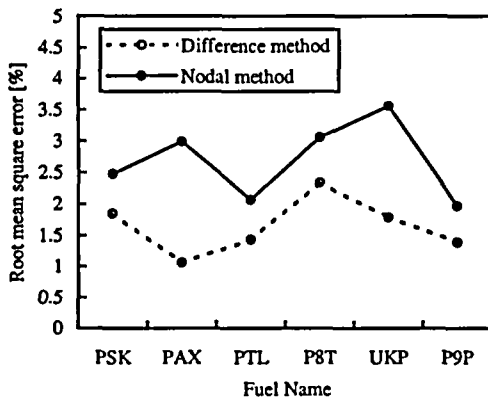


Fig. 18 Comparison of rms errors of axial power distribution between difference method and nodal method (15th cycle)

and 19. The comparisons of fuel assembly power and burnup between calculation and measurement are shown in Figs. 20 and 21.

The accuracy of POLESTAR code with finite difference method was as follows. The rms errors of calculated axial power distributions were less than 2.3% and the rms errors of calculated axial burnup distributions were less than 2.7% compared with the γ -scanning data. The rms error of calculated fuel assembly power was 4.5% and the rms error of calculated fuel assembly burnup was 3.4% compared with the γ -scanning data.

On the other hand, the accuracy of POLESTAR code with modern nodal method was as follows. The rms errors of calculated axial power distributions were less than 3.6% and the rms errors of calculated axial burnup distributions were less than 2.2% compared with the γ -scanning data. The rms error of calculated fuel assembly power was 3.7% and the rms error of calculated fuel assembly burnup was 2.3% compared with the γ -scanning data.

b) Evaluation of POLESTAR Code by 16th Cycle γ -scanning Data

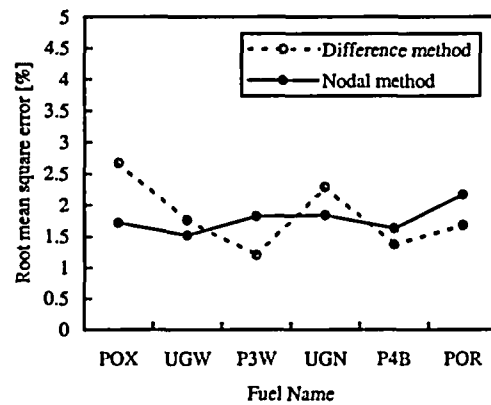


Fig. 19 Comparison of rms errors of axial burnup distribution between difference method and nodal method (15th cycle)

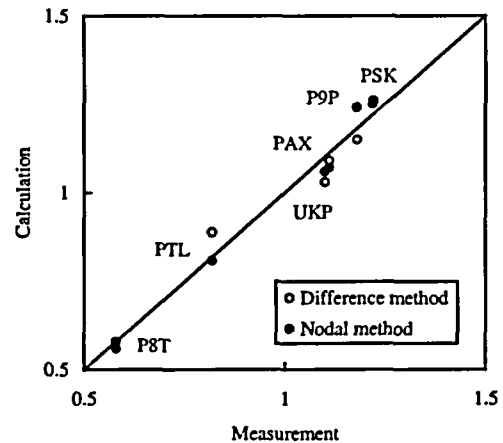


Fig. 20 Comparison of fuel assembly power between calculation and measurement (15th cycle)

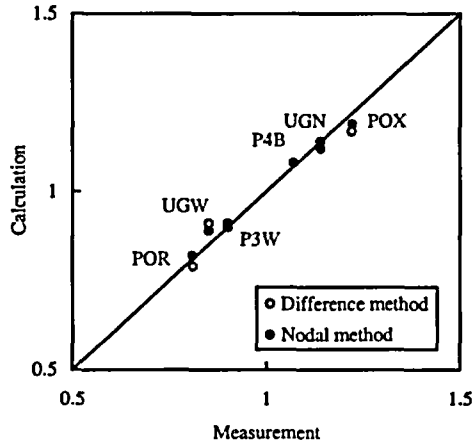


Fig. 21 Comparison of fuel assembly burnup between calculation and measurement (15th cycle)

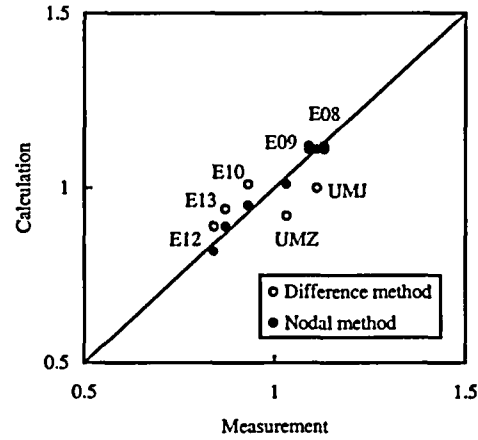


Fig. 23 Comparison of fuel assembly power between calculation and measurement (16th cycle)

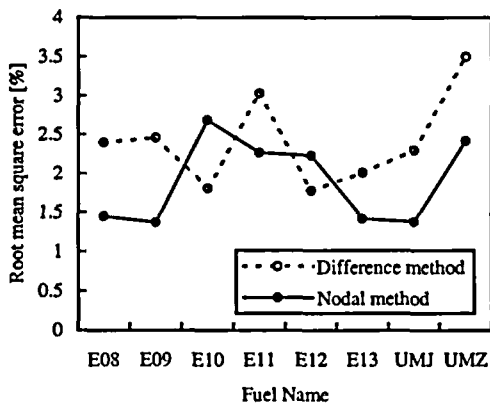


Fig. 22 Comparison of rms errors of axial power distribution between difference method and nodal method (16th cycle)

Table 4 Summary of the calculation accuracy analyzed by γ -scanning

		Difference method	Nodal method
15th cycle	Averaged rms error of power distribution (%)	Axial 1.7	Radial 2.8
	Averaged rms error of burnup distribution (%)	Axial 4.5	Radial 3.7
		Axial 1.9	Radial 1.8
16th cycle	Averaged rms error of power distribution (%)	Axial 2.5	Radial 1.8
		Axial 7.6	Radial 2.3

The rms errors of calculated axial power distribution with respect to the measurement are shown in Fig. 22 and the comparisons of fuel assembly power between calculation and measurement are shown in Fig. 23.

The accuracy of POLESTAR code with finite difference method was as follows. The rms errors of calculated axial power distributions were less than 3.5% and the rms error of calculated fuel assembly power was 7.6% compared with the γ -scanning data.

On the other hand, the accuracy of POLESTAR code with modern nodal method was as follows. The rms errors of calculated axial power distributions were less than 2.7% and the rms error of calculated fuel assembly power was 1.8% compared with the γ -scanning data.

The results of evaluation of POLESTAR code are summarized in Table 4. The accuracy of POLESTAR code with modern nodal method is better than that of POLESTAR code with finite difference method.

(3) Comparison of Effective Multiplication Factor (k_{eff})

The histogram of k_{eff} , which corresponds to the critical states during full power operation, calculated by POLESTAR

code with finite difference method is shown in Fig. 24. The averaged k_{eff} is 0.991 and its standard deviation (1σ) is 0.002. On the other hand, the histogram of k_{eff} calculated by POLESTAR code with modern nodal method is shown in Fig. 25. The averaged k_{eff} is 1.000 (theoretical value) and its standard deviation is 0.002. The difference in the averaged k_{eff} between finite difference method and modern nodal method is 0.9% Δk . The standard deviation of the k_{eff} is the same, i.e., 0.2% Δk for finite difference method and modern nodal method. The accuracy of POLESTAR code with modern nodal method is better than that of POLESTAR code with finite difference method.

(4) Void Reactivity Coefficient

The void reactivity coefficient at about 40% power level is obtained by analyzing the transient behavior of the reactor power when the RCP speed changes from 450 to 900 rpm. The transient behavior is undergone according to the following procedures. Firstly, RCP flow increases to almost double and the void fraction decreases rapidly. Secondly, the reactor power changes a little and the automatic rods are inserted to keep the reactor power constant. This is because void reactivity is very small and the reactor power is well controlled by automatic rods. The void reactivity coefficient is evaluated by the changes of void fraction and the position of automatic rods. The prediction errors of calculated void reactivity coef-

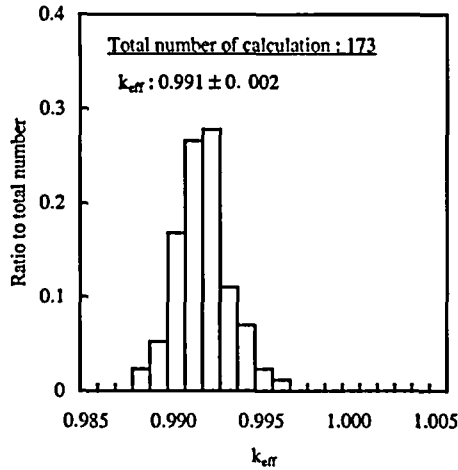


Fig. 24 Histogram of k_{eff} calculated by POLESTAR (difference method)

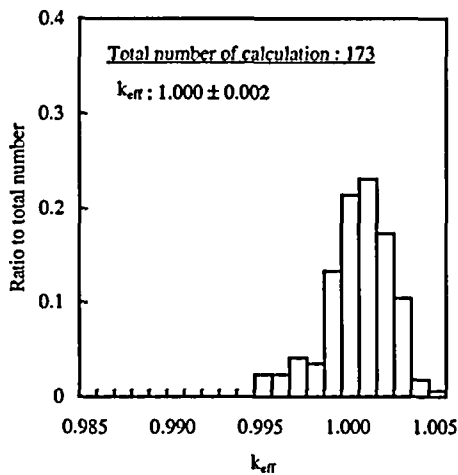


Fig. 25 Histogram of k_{eff} calculated by POLESTAR (nodal method)

efficient with respect to the measurement (evaluated void reactivity coefficient) are shown in Fig. 26. The prediction error of void reactivity coefficient is $\pm 3 \times 10^{-5} \Delta k/k/\% \text{void}$ for the equilibrium cores.

(5) Power Coefficient

The power coefficient at 100% power level is obtained by analyzing the change of reactor power when the one control rod is inserted about 3% to full strokes. The power coefficient is evaluated by the changes of power and the position of control rod. The prediction errors of calculated power coefficient with respect to the measurement (evaluated power coefficient) are shown in Fig. 27. The prediction error of power coefficient is $\pm 1.5 \times 10^{-5} \Delta k/k/\% \text{power}$ for POLESTAR code with modern nodal method.

V. Conclusion

The ATR type core design code system WIMS-ATR/POLESTAR has been developed. For the purpose of accu-

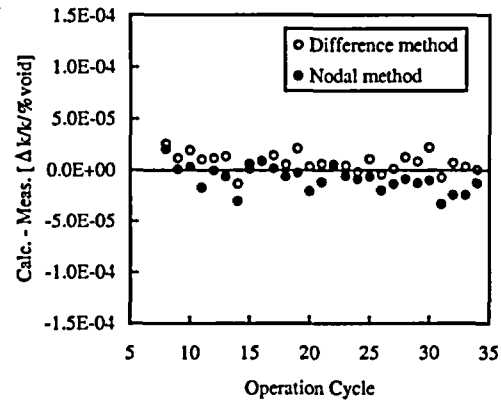


Fig. 26 Comparison of void reactivity coefficient differences between calculation and estimated measurement

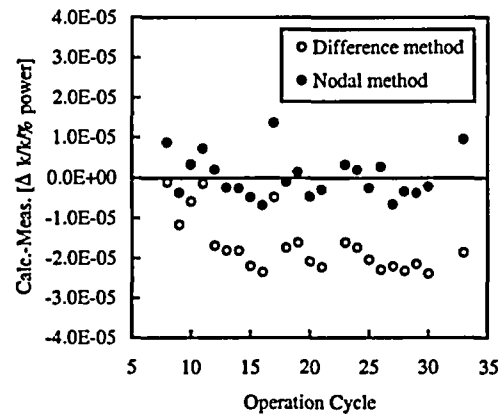


Fig. 27 Comparison of power coefficient differences between calculation and estimated measurement

racy improvement, it is taken account of the differences of isotopic composition of the plutonium, ^{241}Pu γ -decay, and ^{241}Am accumulation. Furthermore, the modern nodal method with JENDL-3.2 nuclear data library is installed in this code system for the purpose of additional accuracy improvement.

The accuracy of this code system also has been evaluated by means of operational data such as thermal neutron flux distributions, on-site γ -scanning data, effective multiplication factor, void reactivity coefficient and power coefficient. The accuracy of modern nodal method for thermal neutron flux distributions is less than that of finite difference method. The accuracy of modern nodal method for void reactivity coefficient is nearly equal to finite difference method. The accuracy of modern nodal method for on-site γ -scanning data, effective multiplication factor and power coefficient is better than that of finite difference method.

Acknowledgments

The authors would like to express their gratitude to Kuniyoshi Saito of CRC Solutions Co., Ltd. for his programming and detailed evaluation work on WIMS-ATR/POLESTAR code system and Hitoshi Kawashima of

Tsuruga Atomic Service Co., Ltd. for his support work on FUGEN's core management. They are also grateful to Mitsuo Matsumoto of Japan Nuclear Cycle Development Institute for his advice on data evaluation and the members who have been engaged in FUGEN's core management.

References

- 1) S. Sawai, T. Haga, M. Akebi, *et al.*, "Fugen HWR reaches commercial operation," *Nucl. Eng. Int.*, **24**, 33 (1979).
 - 2) S. Ohteru, *et al.*, "Core management of the Prototype Advanced Thermal Reactor Fugen," *PNC Technical Report.*, No. 44, (1982).
 - 3) M. Matsumoto, *et al.*, "Core design and characteristics of Fugen," *PNC Technical Report.*, No. 65, (1988).
 - 4) S. Sawai, *et al.*, "Characteristics of plutonium utilization in the Heavy Water Moderated, Boiling Water Cooled Reactor ATR," *Nucl. Eng. Des.*, **125**, 251 (1991).
 - 5) Y. Shiratori, T. Furubayashi, M. Matsumoto, "Operating experience with MOX fuel loaded heavy water reactor," *J. Nucl. Sci. Technol.*, **30**[1], 78 (1993).
 - 6) T. Iijima, *et al.*, "Characteristics of plutonium utilization in the Heavy Water Moderated, Boiling Light Water Cooled Reactor Fugen," *Proc. IAEA Specialists Meeting on Advances in Heavy Water Reactors*, Toronto, Canada, June 7-10, 1993, p. 96 (1993).
 - 7) T. Nakagawa, *et al.*, *J. Nucl. Sci. Technol.*, **32**[12], 1259 (1995).
 - 8) J. R. Askew, *et al.*, *J. Brit. Nucl. Eng. Soc.*, **5**, 564 (1966).
 - 9) H. Honeck, *Trans. Am. Nucl. Soc.*, **5**, 47 (1962).
 - 10) T. Haga, N. Aihara, H. Kamikawa, "POLESTAR-2F/3F code for POWER mapping and refueling analyses of HWR-Fugen," *Proc. Specialists Meeting on Calculation of 3-Dimensional Rating Distributions in Operating Reactors*, Paris, France, Nov. 26-28, 1979, NEA-OECD Special Publication, p. 319 (1980).
 - 11) H. Kato, T. Haga, S. Ohteru, "Core management analysis of the Fugen Heavy Water Moderated Plutonium Uranium Mixed Oxide Reactor," *Nucl. Sci. Eng.*, **87**, 361 (1984).
-